The effect of Bisphenol A vs Bisphenol F on the performance of polysulfone membranes

Supporting Information: Polymer Thermal Data, Additional Solution Rheology Data, 40 kDa pBPA Membrane Thickness Comparison, ^{1}H NMR Spectroscopy with integrations, Additional Comparison of Solvent Permeance to Solvent Density, Molecular Diameter, Carbon Number, and the distance between solvent and polymer HSPs

Authors: Taysha Telenar [a,b], Rowen Sadlier [c], Kelly Nguyen [a,b], Alexis Powell [d], Oshio Oyageshio [e], Matthew Green [a,b]

a. Department of Chemical Engineering, School for Engineering of Matter, Transport and Energy, Arizona State University, Tempe, Arizona 85281, USA
b. Biodesign Center for Sustainable Macromolecular Materials and Manufacturing, Arizona State University, Tempe, AZ 85281, USA
c. Department of Chemical Engineering, Albert Nerken School of Engineering, The Cooper Union for the Advancement of Science and Art, New York City, NY, 10003, USA
d. Department of Chemical and Biomolecular Engineering, School of Engineering and Applied Science, University of Pennsylvania, Philadelphia, PA 19104, USA
e. Department of Chemical Engineering, College of Engineering, University of Massachusetts Amherst, Amherst, MA 01003, USA

Thermal Properties:

Figure S1 & Table S1 show the TGA data, DSC data for each polymer, and their thermal transitions.

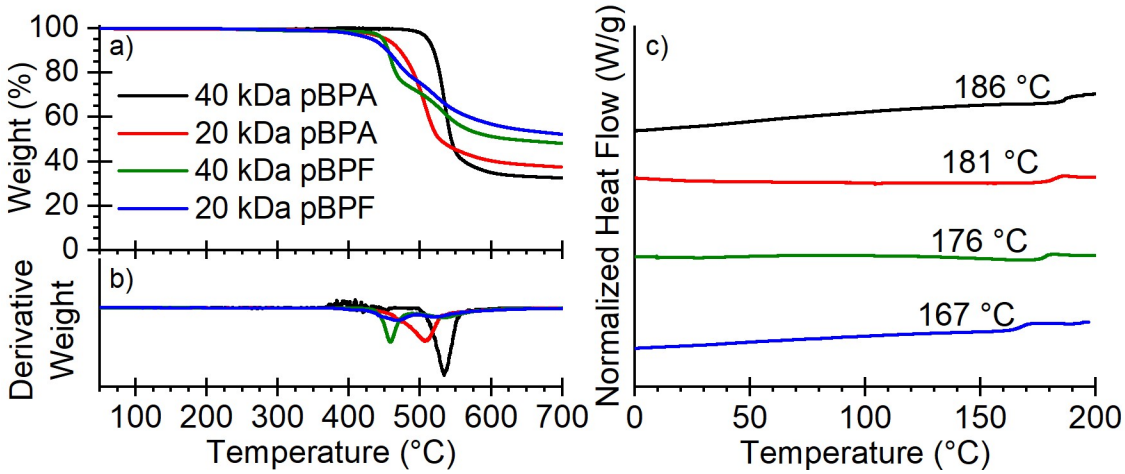

Figure S1: a) TGA of each polymer and b) derivation curves support them. C) DSC for each polymer shows an increase in Tg with increased molecular weight of pBPF from 167 to 176 °C.

Table S1: Additional TGA & DSC Data for Comparison

Polymer	$T_{d,5\%}$	Derivative Peaks		Char Yield	T_g
	°C	°C		wt. %	°C
20 kDa pBPF	434	468	522	51.3 %	167
40 kDa pBPF	453	464	543	45.0 %	176
20 kDa pBPA	453	507		37.7 %	181
40 kDa pBPA	511	534		31.6 %	186

Solution Rheology:

Steady state solution rheology, in **Figure S2a-d**, shows an increase in viscosity as polymer loading is increased. Additionally, higher molecular weight polymers showed a wider gap between loadings, leading to higher viscosities overall. Notably, 40 kDa pBPF shows shear thinning at 30 wt.% loading.

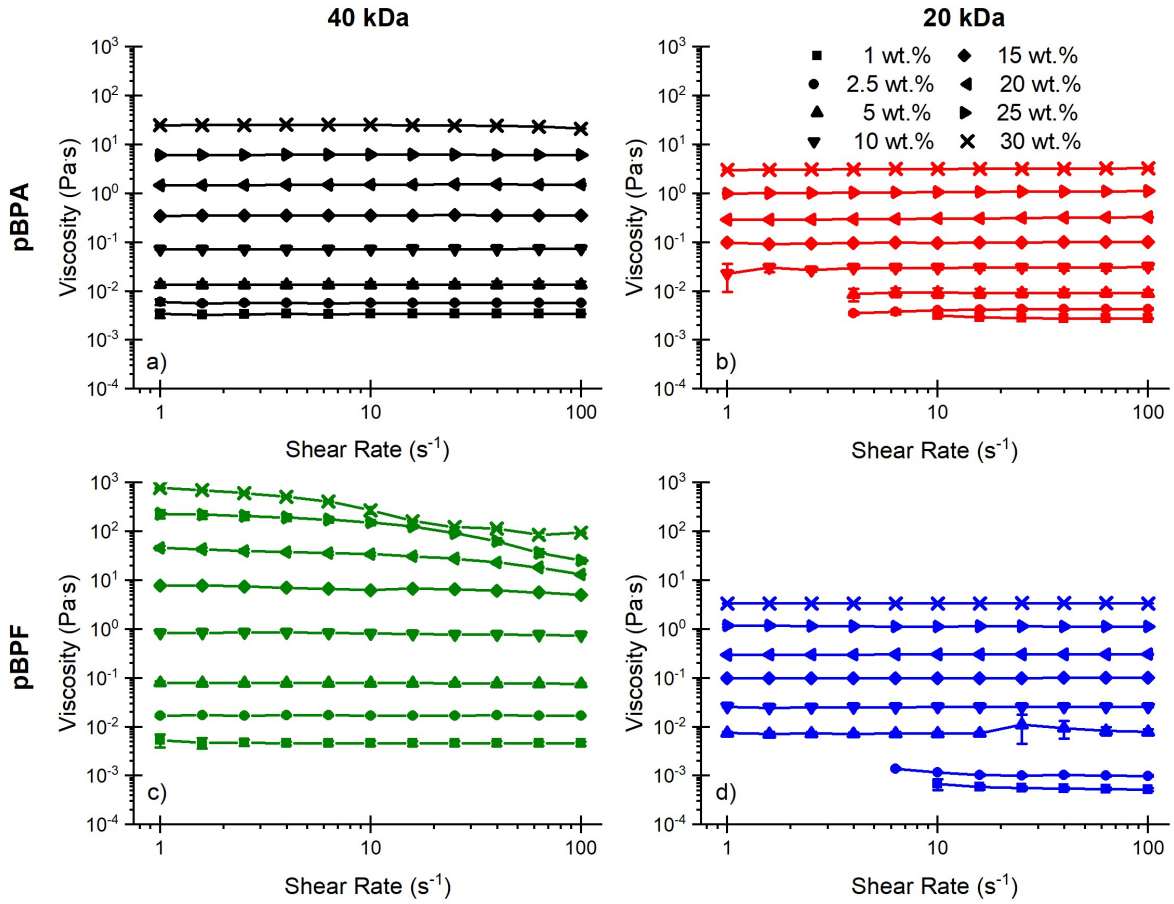

Figure S2: Solution viscosity from cone-plate rheology for a) 40 kDa pBPA, b) 20 kDa pBPA, c) 40 kDa pBPF, and d) 20 kDa pBPF shows an increase in viscosity as polymer concentration increases. 40 kDa pBPF shows shear thinning at 30 wt.% polymer loading.

40 kDa pBPA Membrane Thickness Comparison:

DI water permeance tests in **Figure S3** for 40 kDa pBPA show that as thickness increases, permeance can decrease significantly for higher polymer loading.

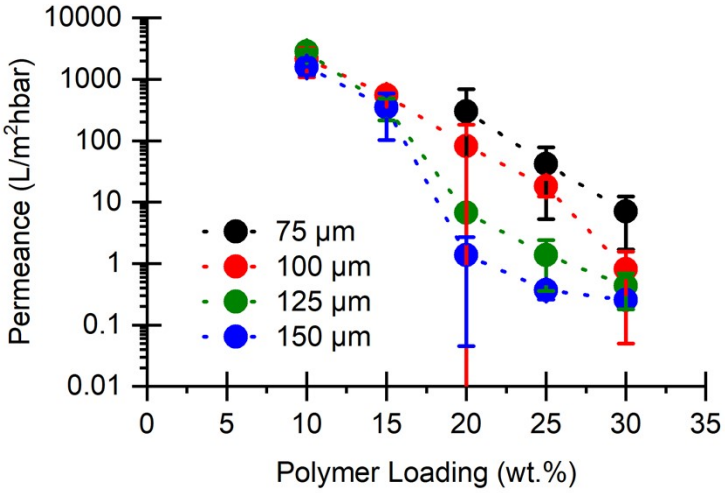

Figure S3: 40 kDa pBPA membranes made at 75, 100, 125, and 150 µm and tested at 5 bar show a decrease in permeance as thickness is increased.

[1]H NMR Spectroscopy with integrations:

Figures S4 & S5 show integrations and peak locations for each 1H NMR Spectroscopy peak.

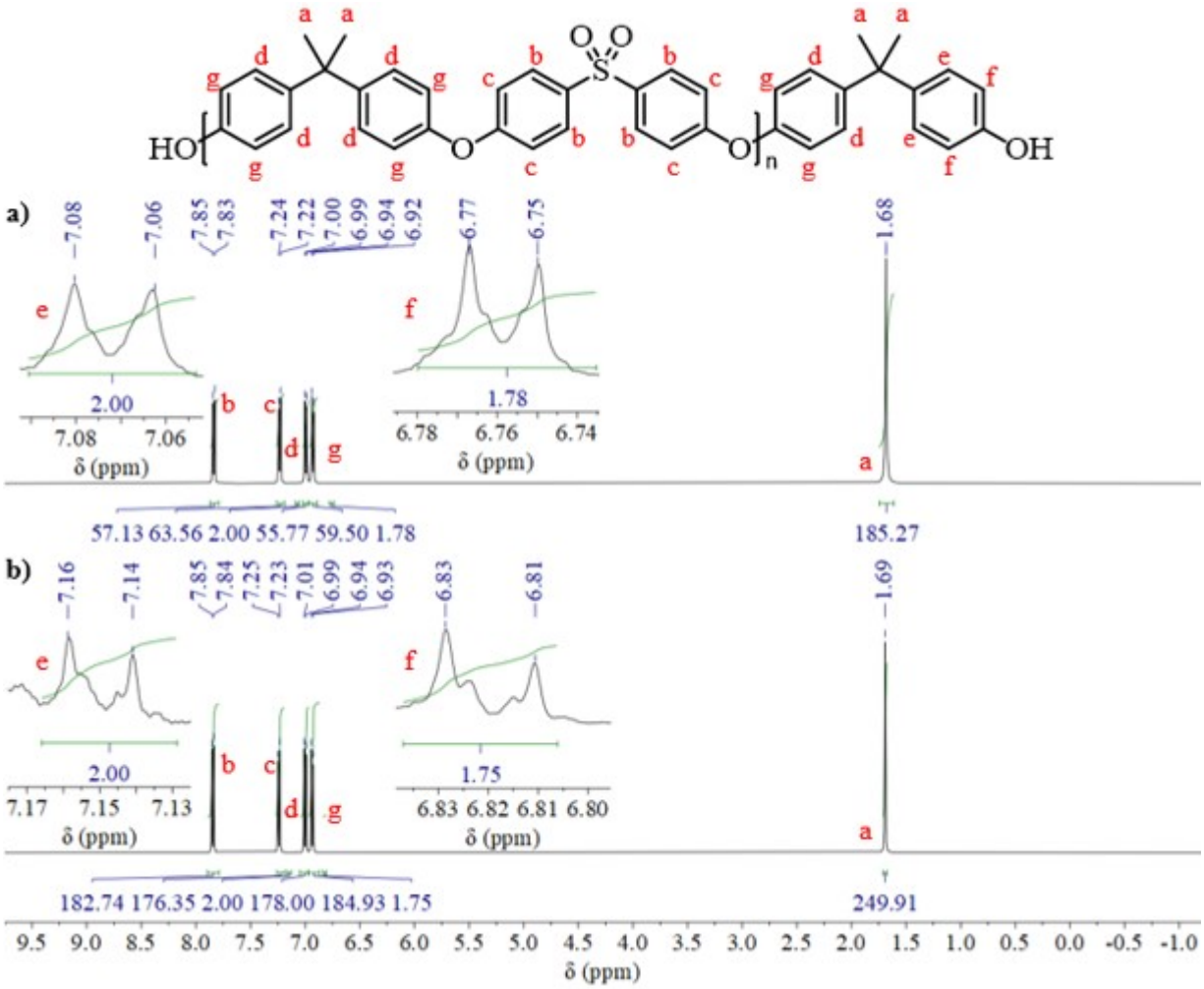

Figure S4: [1]H NMR Spectroscopy for **a)** 20 kDa pBPA confirms 14.4 kDa and **b)** 40 kDa pBPA confirms 42.6 kDa.

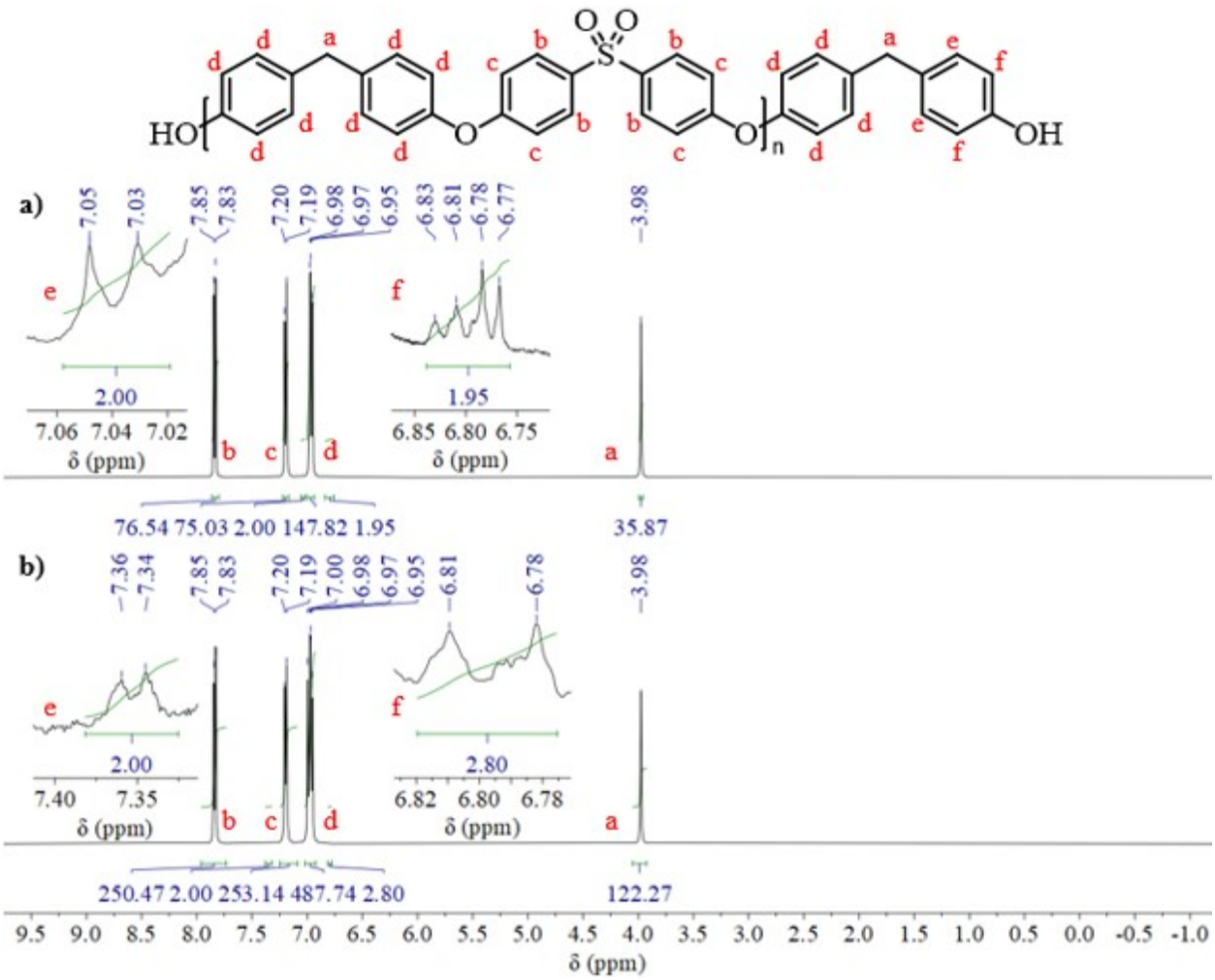

Figure S5: ^{1}H NMR Spectroscopy for **a)** 20 kDa pBPF confirms 16.1 kDa and **b)** 40 kDa pBPF confirms 43.7 kDa.

Solvent Permeance vs. Solvent Density, Molecular Diameter, Carbon Number, and The Distance Between Solvent & Polymer HSPs:

Figure S6 shows the lack of trends observed when comparing solvent permeance to solvent density, molecular diameter, number of carbon atoms, and distance between polymer and solvent HSPs.

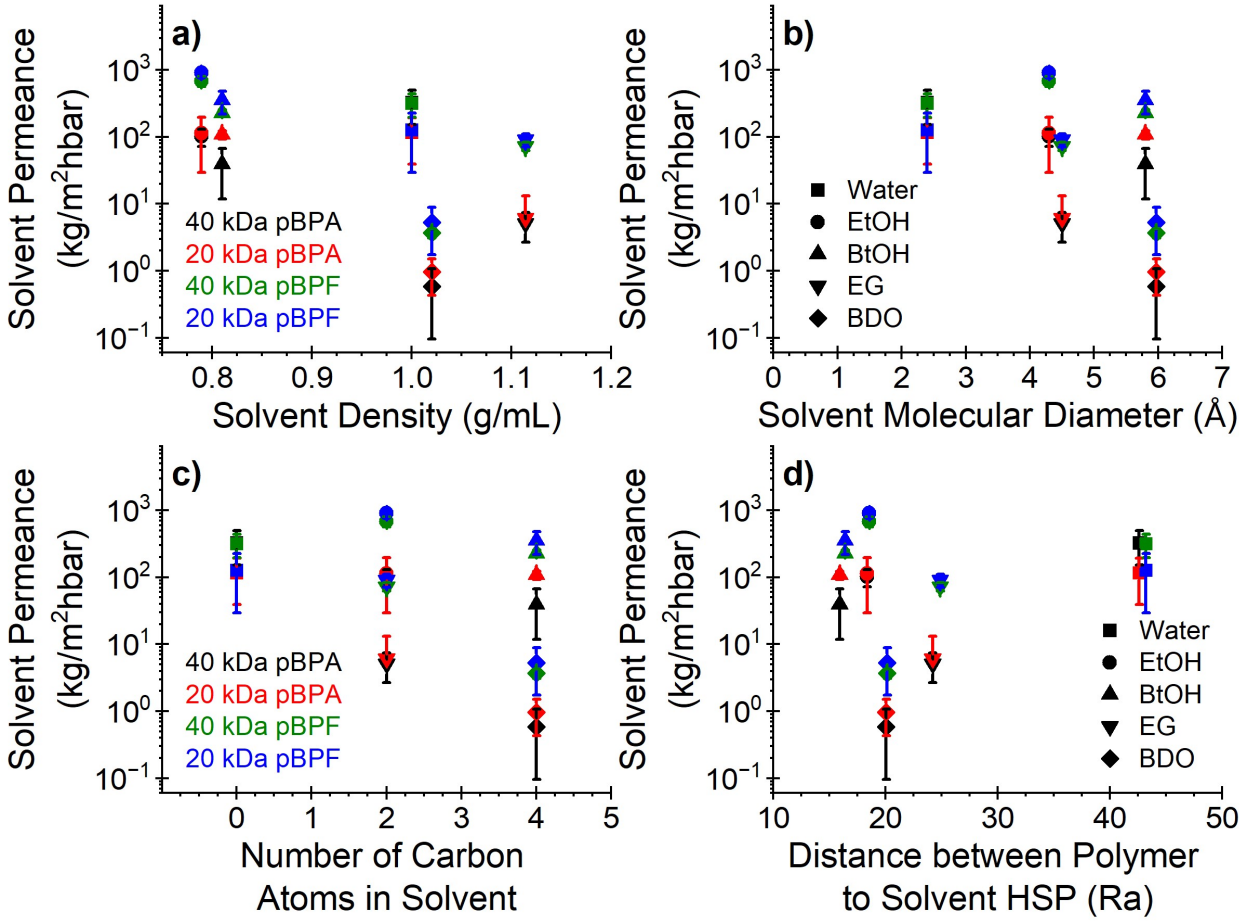

Figure S6: Solvent permeance compared to solvent **a)** density,[1–5] **b)** molecular diameter,[6–10] **c)** carbon number of solvent, and **d)** distance between polymer and solvent HSP[11–13] at a transmembrane pressure drop of 5 bar for water, EtOH, BtOH, EG, and BDO through membranes cast from 15 wt.% polymer solutions.

(1) Kong, L.; Li, B.; Zhao, L.; Zhang, R.; Wang, C. Density, Viscosity, Surface Tension, Excess Property and Alkyl Chain Length for 1,4-Butanediol (1) + 1,2-Propanediamine (2) Mixtures. *J. Mol. Liq.* **2021**, *326*. https://doi.org/10.1016/j.molliq.2020.115107.

(2) Torín-Ollarves, G. A.; Segovia, J. J.; Martín, M. C.; Villamañán, M. A. Thermodynamic Characterization of the Mixture (1-Butanol + Iso-Octane): Densities, Viscosities, and Isobaric Heat Capacities at High Pressures. *J. Chem. Thermodyn.* **2012**, *44* (1), 75–83. https://doi.org/10.1016/j.jct.2011.08.012.

(3) The Engineering Toolbox. *Water Density, Specific Weight and Thermal Expansion Coefficients - Temperature and Pressure Dependence*. https://www.engineeringtoolbox.com/water-density-specific-weight-d_595.html (accessed 2025-01-11).

(4) The Engineering Toolbox. *Ethanol - Density and Specific Weight vs. Temperature and Pressure*. https://www.engineeringtoolbox.com/ethanol-ethyl-alcohol-density-specific-weight-temperature-pressure-d_2028.html (accessed 2025-01-11).

(5) Merck & Co. Ethylene Glycol. In *The Merck index: An encyclopedia of chemicals, drugs, and biologicals*; O'Neil, MJ; Smith, A; Heckelman, PE; Obenchain, JR, Jr; Gallipeau, JAR; D'Arecca, MA; Budavari, S., Ed.; Whitehouse Station, NJ, 2001; pp 3832–3833.

(6) Lemmon, E. W.; Bell, I. H.; Huber, M. L.; McLinden, M. O. *Thermophysical Properties of Fluid Systems*, 20899th ed.; Mallard, W. G., Linstrom, P. J., Eds.; National Institute of Standards and Technology: Gaithersburg, MD, 2023. https://doi.org/https://doi.org/10.18434/T4D303.

(7) Rayabharam, A.; Qu, H.; Wang, Y.; Aluru, N. R. Spontaneous Sieving of Water from Ethanol Using Angstrom-Sized Nanopores. *Nanoscale* **2023**, *15*, 12626–12633. https://doi.org/10.1039/d3nr02768f.

(8) Hu, C.; Guo, R.; Li, B.; Ma, X.; Wu, H.; Jiang, Z. Development of Novel Mordenite-Filled Chitosan – Poly (Acrylic Acid) Polyelectrolyte Complex Membranes for Pervaporation Dehydration of Ethylene Glycol Aqueous Solution. *J. Memb. Sci.* **2007**, *293*, 142–150. https://doi.org/10.1016/j.memsci.2007.02.009.

(9) Kumar, P.; Varanasi, S. R.; Yashonath, S. Relation Between the Diffusivity, Viscosity, and Ionic Radius of LiCl in Water, Methanol, and Ethylene Glycol: A Molecular Dynamics Simulation. *J. Phys. Chem. B* **2013**, *117*, 8196–8208. https://doi.org/10.1021/jp4036919.

(10) Rigo, E.; Dong, Z.; Park, J. H.; Kennedy, E.; Hokmabadi, M.; Almonte-garcia, L.; Ding, L.; Aluru, N.; Timp, G. Measurements of the Size and Correlations between Ions Using an Electrolytic Point Contact. *Nat. Commun.* **2019**, *10* (2382), 1–13. https://doi.org/10.1038/s41467-019-10265-2.

(11) Abbott, S. *HSP Basics*. Practical Solubility. https://www.stevenabbott.co.uk/practical-solubility/hsp-basics.php (accessed 2025-01-11).

(12) Stefanis, E.; Panayiotou, C. Prediction of Hansen Solubility Parameters with a New Group-Contribution Method. *Int. J. Thermophys.* **2008**, *29* (2), 568–585. https://doi.org/10.1007/s10765-008-0415-z.

(13) Enekvist, M.; Liang, X.; Zhang, X.; Dam-Johansen, K.; Kontogeorgis, G. M. Estimating Hansen Solubility Parameters of Organic Pigments by Group Contribution Methods. *Chinese J. Chem. Eng.* **2021**, *31*, 186–197. https://doi.org/10.1016/j.cjche.2020.12.013.